Journal of Alloys and Compounds 788 (2019) 283–288

Contents lists available at ScienceDirect

Journal of Alloys and Compounds

journal homepage: http://www.elsevier.com/locate/jalcom

Tunability of correlated magnetocaloric effect and magnetoresistance by Ar ion irradiation in a Gd-based nanocrystalline/amorphous alloy

Qiang Luo [a, b, *], Xiaodong Zhang [c], Baolong Shen [a, b, d, **]

[a] School of Materials Science and Engineering, Southeast University, Nanjing 211189, China
[b] Jiangsu Key Laboratory for Advanced Metallic Materials, Nanjing 211189, China
[c] School of Material Science and Engineering, Harbin Institute of Technology, Harbin 150001, China
[d] Institute of Massive Amorphous Metal Science, China University of Mining and Technology, Xuzhou 221116, China

ARTICLE INFO

Article history:
Received 21 January 2019
Received in revised form
17 February 2019
Accepted 19 February 2019
Available online 20 February 2019

Keywords:
Magnetic entropy change
Microstructure
Irradiation
Magnetoresistance

ABSTRACT

The magnetocaloric effect and magnetoresistance (MR) of nanocrystalline/amorphous $Gd_{65}Co_{15}Al_{10}Zr_{10}$ alloy were investigated. The as-spun alloy shows a large maximum magnetic entropy change (MEC) of 5.4 $Jkg^{-1}K^{-1}$ under a field change of 5 T and a refrigerant capacity of 468.9 Jkg^{-1}. It is found that Ar ion irradiation increases the MEC and refrigerant capacity (RC) of the alloy, which is associated with the anisotropic stress and heating effects, increasing the atomic mobility and short-range order around Gd. Moreover, the maximum MEC shows a power-law (linear) relationship with the MR above (below) the Curie temperature for the as-spun ribbon, which alters after irradiation.

The magnetocaloric effect, characterized by the temperature change of a magnetic solid when exposed to an external magnetic field variation, is closely related to its atomic and magnetic structures. During the last several decades, intense research activities were devoted to developing various kinds of magnetocaloric materials with large magnetic entropy change (MEC) [1–10]. And most of the efforts were previously focused on the crystalline magnetocaloric materials, especially those with first order structural/magnetic transition, which may show giant magnetocaloric effect [1–5]. Nevertheless, in these materials the giant MEC usually occurs in a very narrow temperature range and usually some non-desirable effects such as poor mechanical and thermal stability, and magnetic hysteresis exist [1–4]. Magnetic materials with second order magnetic transition usually show moderate maximal MEC ($-\Delta S_m$), but with a broad MEC peak, which may produce very high refrigerant capacity (RC) [8,9]. Recently, amorphous alloys (AMs) with a second order transition have been attracting worldwide research interest due to their many magnetic/electronic/mechanical advantages [8–17]. Many publications investigated the effects of composition, crystallization, hydrogenation, magnetic anisotropy and effective magnetic moment on the magnetocaloric performance of Fe-based and rare earth based metallic glasses in ribbon, bulk rod and wire-shaped forms [8–20]. To further enhance RC, composites were also fabricated by stocking two or more kinds of amorphous alloy ribbons layer by layer in a proper weight fraction to obtain materials with a table-like MEC response [21]. In addition, in-situ formed two-phase or multi-phase magnetic composite systems are attracting increasing interest. And in situ formed composite materials with high RC were reported in several rare-earth-based alloys: Gd-Al-Mn, Gd-Fe-Al and Gd-Co-Al [22–24]. Despite some progress in exploring the MEC of amorphous alloys and related composites, the nature of their magnetocaloric behavior is still poorly understood due to the structural/magnetic complexity. And for practical reason the magnetocaloric performance of AMs and their composites requires urgently to be further improved to make them more competitive.

In this Letter, we explored the microstructure, magnetocaloric response and magnetoresistance (MR) of the $Gd_{65}Co_{15}Al_{10}Zr_{10}$ melt-spun ribbon, particularly the effects of Ar ion irradiation. The ribbon shows amorphous/nanocrystalline composite structure and two magnetic transitions. During Ar ion irradiation, the combination of anisotropic stress and heat induces change of morphology,

* Corresponding author. School of Materials Science and Engineering, Southeast University, Nanjing 211189, China.
** Corresponding author. School of Materials Science and Engineering, Southeast University, Nanjing 211189, China.
E-mail addresses: q.luo@seu.edu.cn (Q. Luo), blshen@seu.edu.cn (B. Shen).

https://doi.org/10.1016/j.jallcom.2019.02.224
0925-8388/

atomic arrangement and structure ordering of the surface layer. Importantly, obvious improvement of magnetocaloric performance by irradiation has been obtained. Moreover, the maximal MEC is found to correlate uniquely with the MR in both the as-spun and irradiated ribbons, which is different from the relationships of some reported crystalline and amorphous solids. These findings are of significance for fundamental research and potential applications of amorphous and nanocrystalline alloys.

The alloy ingot with nominal composition of $Gd_{65}Co_{15}Al_{10}Zr_{10}$ was first prepared by arc melting technique in a Ti-gettered argon atmosphere. Then the glassy ribbons with a thickness of ~30 μm and a width of ~4 mm were fabricated by using single roller melt-spinning method. The microstructure of the ribbon was checked by x-ray diffraction (XRD) using D/MAX2550VB3+/PC diffractometer with Cu Kα radiation, and transmission electron microscopy (TEM; JEM-2100F) operated at 200 kV. The magnetization and resistivity were measured using a physical properties measurement system, PPMS 6000 of Quantum Design Company. The Ar ion irradiation with energy of 170 kev was performed on an ion beam irradiation system. During irradiation process, the specimens were placed in a vacuum of ~1.33×10^{-2} Pa. The ion fluence of 1.0×10^{15} was obtained. The atomic force microscope (AFM, SeikoSPA300HV, Japan) was used to observe the surface morphology of the as-spun and irradiated ribbons.

The XRD patterns of the as-spun and irradiated alloys are shown in Fig. 1, which show the composite structure of both alloys. Irradiation does not alter the main feature of XRD pattern, but small change can be detected, such as the position and width of the first sharp diffraction peak and its neighboring peak (the inset of Fig. 1 (a)). This indicates that irradiation induces rearrangement of atoms of the sample. Both the as-spun and irradiated ribbons show amorphous plus crystalline composite structure, which can be indicated from the TEM results of the irradiated ribbon as an example (shown in Fig. 1). In addition, by using the Debye-Scherrer equation the average grain size is determined to be 19.2 nm and 22.2 nm for the as-spun and irradiated samples, respectively, indicating the growth of nanocrystals in the surface layer due to the heating effect. As the Ar ions bombard the ribbon sample, their kinetic energy partly converts into heat and the momentum can convert into force, which may lead to nucleation and growth of nanocrystals in the alloy [25]. The average modulus and hardness from the Nano-indentation experiments are 60.3 GPa and 3.58 GPa,respectively for the as-spun sample. And after irradiation, they increase slightly to 61.8 GPa and 3.63 GPa, respectively at a depth of ~1.0 μm, indicating the hardening effect of irradiation. The surface morphology of the pristine (Fig. 1(c–e)) as well as the irradiated (Fig. 1(f–h)) ribbons is shown in Fig. 2. From the AFM images, mound-like structure can be clearly seen in the as-spun ribbon surface, which is related to the island like growth of nanocrystals during melt spinning process. Obviously, Ar ion irradiation changes the surface features and remarkably damages those mounds found in the pristine ribbon (Fig. 1(f–h)). The surface roughness is determined to be 88.5 nm and 15.8 nm for the as-spun and the irradiated ribbons, respectively, indicating the smoothening of the surface upon irradiation. Note that we use a low energy of 170 kev for irradiation experiment, which has the advantage of modifying only the surface layer leaving the bulk unaltered.

To further understand the impact of irradiation on the

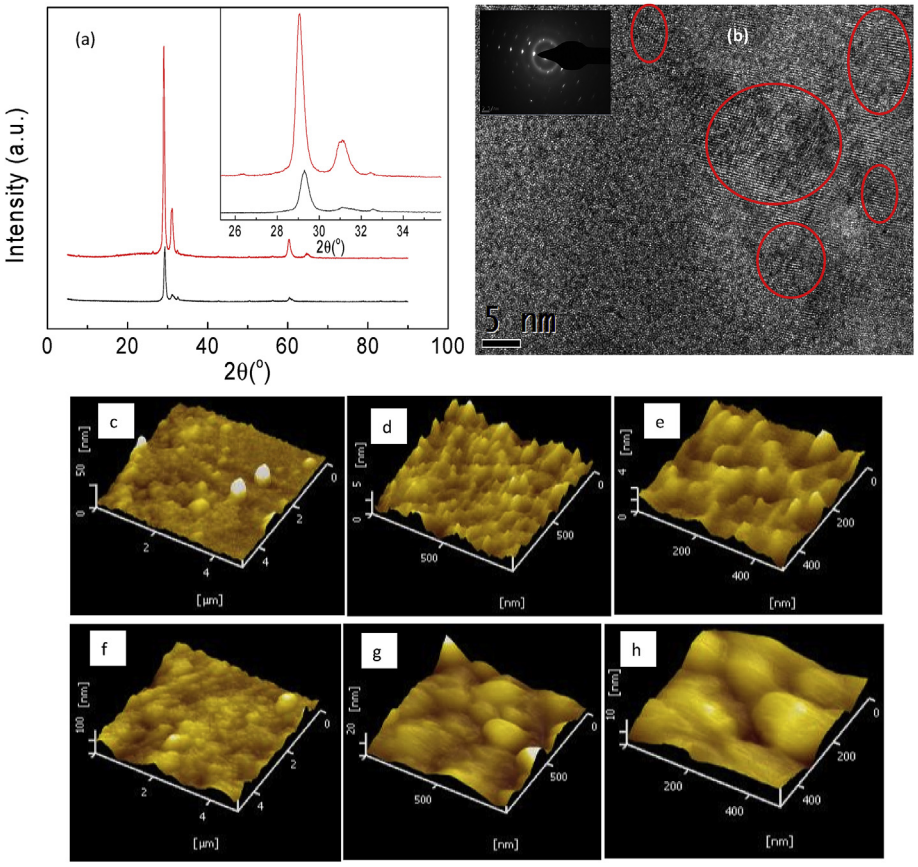

Fig. 1. (a) XRD patterns of the as-spun (lower curve) and Ar irradiated (upper curve) alloys, the inset shows the enlarged part around the first diffraction peak. (d) High-resolution TEM of the irradiated ribbon showing the amorphous plus nanostructured composite nature. And AFM images of the as-spun (c–e) and Ar ion irradiated alloys (f–h).

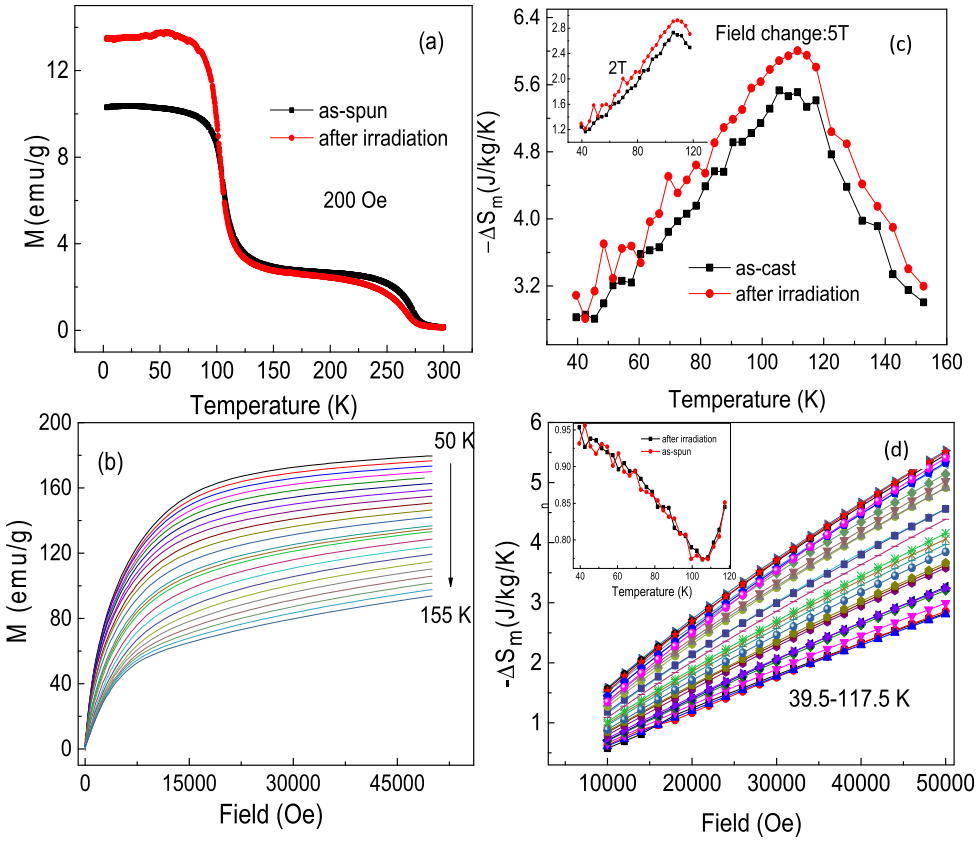

Fig. 2. (a) Temperature dependence of the magnetization under 200 Oe for the alloys. (b) Isothermal magnetization curves at a set of temperatures for the as-spun ribbon. (c) MEC under a field change of 5 T for both ribbons. The inset shows the MEC under a field change of 2 T. (d) Field dependence of the magnetic entropy change of the as-spun alloy, the inset shows the temperature dependence of the *n* value.

magnetization and magnetocaloric effect, magnetic measurements were carried out. Fig. 2(a) presents the temperature dependence of magnetization under a magnetic field of 200 Oe, which was measured on heating after initially cooling to 2 K in 200 Oe. Both alloys show clearly double magnetic transitions, which indicates that the irradiation does not change the composite nature. The lower magnetic transition mainly arises from the amorphous phase and the higher magnetic transition mainly comes from the nano-structured phase(s). Nevertheless, clear change of the magnetization after irradiation can still been observed. After irradiation, the magnetic transition around 270 K gets smoothed, and especially the low temperature magnetization (below 100 K) increases considerably (roughly from 10 emu/g to 14 emu/g). It is well known that the magnetic/mechanical properties of amorphous/nanocrystalline composite materials depend strongly on their local structure/property, like local strain, grain size/shape, amorphous-nanocrystalline interface, defects, *etc*. Therefore, the change of magnetic behaviors of the ribbon after Ar ion irradiation should relate to stress relaxation and local atom arrangement induced by irradiation. The high-energy Ar ions bombarding the ribbons will engender heat along with a perpendicular force on the atoms of the ribbon, which promotes atomic diffusion and deformation, and thereby causes structure relaxation and atomic short-range ordering. During this process, the change of Gd-Gd distance and local environment around Gd may result in the increase of magnetization after irradiation.

Fig. 2(b) displays a set of isothermal *M-H* curves of the as-quenched ribbon (as an example) from 0 to 50 kOe, from which the MEC of the sample can be determined from the thermodynamic Maxwell relations. To ensure that each magnetization curve was measured isothermally, the sweeping rate was slow enough during the measurement. From the Maxwell equation, a maximum MEC can be obtained near the magnetic transition temperature where the magnetization varies sharply with temperature in a constant field. Sharper change of the magnetization around 100 K for the irradiated sample (Fig. 2(a)) implies its larger maximum MEC than that of the as-spun ribbon. From Fig. 2 (b) it is observed that below ~1.5T, the magnetization increases more slowly with increasing field than that of typical Gd-based metallic glasses due to the muti-phase nature of present alloys [8], which obstructs the magnetization process of the sample.

Fig. 2(c) shows the $-\Delta S_m$ as a function of temperature under 5T for the as-spun and irradiated samples (the inset shows the $-\Delta S_m$ under 2 T). The maxima of $-\Delta S_m$ (under a field change of 5 T) are 5.4 $Jkg^{-1}K^{-1}$ at 105.5 K and 6.0 $Jkg^{-1}K^{-1}$at 111.5 K for the as-spun and irradiated samples, respectively. These values are lower than those of many Gd-based amorphous rod, wire and ribbons [8,14], because of the considerable amount of nanocrystalline phase in present alloys. The well separated Curie temperatures of the amorphous and nanocrystalline phases (around 100 K and 270 K for the amorphous and nanocrystalline phases, respectively) do not lead to broadening of the MEC peak, and thus RC enhancement by the composite structure is not observed here. In contrast, the enhancement of RC in the Nd-Pr-Fe composite was obtained, since the two successive magnetic phase transitions (303 and 332 K) leaded to obvious broadening of the ΔS_m peak. However, these maximum MEC and RC values of present alloys are still larger than those of Fe-based amorphous alloys [1,10]. Present work focuses on

the effect of irradiation on the MEC properties, instead of composition effect. From Fig. 2(c), it is clear that the shape of MEC curve does not change, but the $-\Delta S_m$ values are enhanced clearly in the whole investigated temperature range after irradiation. And the RC value of the as-spun alloy can be determined to be 468.9 Jkg^{-1}, and increases to 511.4 Jkg^{-1} after irradiation. The RC was calculated by numerically integrating the area under the $-\Delta S_m$-T curve, using the temperatures at half-maximum of the peak as the integration limits. The RC values are comparable to the Gd-based metallic glasses [8], and larger than those of the $Gd_5Ge_{1.9}Si_2Fe_{0.1}$ (360 Jkg^{-1}) and $Gd_5Ge_2Si_2$ (305 Jkg^{-1}) alloys [1,2], which are considered as typical magnetic refrigerants. The increase of $-\Delta S_m$ and RC by irradiation is in accordance with the enhancement of magnetization. This is partly related to the local structural relaxation, which decreases the stress-induced anisotropy and eliminates the free-volume and anti-free-volume and other defects. On the other hand, irradiation-induced enhancement of short-range order and atomic mobility may promote the Gd-Gd cluster formation and strengthen the Gd-Gd exchange interactions, which improves the magnetocaloric performances.

For materials with second order magnetic transition, the mean field theory predicted that the field dependent maximal $-\Delta S_m$ at the transition temperature obeyed a power law relationship: $|\Delta S_{Max}| \propto H^n$ [26], where n was ~2/3. Experimentally, n varies from 0.66 to 0.87 for various amorphous alloy systems around the magnetic transition temperature, which implies that n is sensitive to the short to medium range ordered structures of AMs [10,15]. And it was found that a larger degree of inhomogeneity or order in composites can lead to a larger n value [27–29]. Recently, in the Gd-Er-Al-Co AMs it was found that n is related to the degree of magnetic frustration among random magnetic anisotropy and exchange interactions [29]. In present alloy, it is found that the power law fits the data very well in the whole temperature range investigated as shown in Fig. 2 (d) for the as-quenched sample. And both the as-spun and irradiated alloys show similar temperature dependence of n (see the inset of Fig. 2(d)), with their minimal of ~0.77 at 108.5 K (determined under 5 T), which suggests that the irradiation does not change the field dependence behavior of MEC in present alloys. And the larger value of n than the predicted 2/3 around the Curie temperature is related to the composite nature of present alloys. In addition, it was found that for multi-phase materials n decreased with increasing applied field [10]. This implies that larger n values can be obtained when using smaller magnetic field change.

To reveal the relationship between MR and MEC in the Gd-based composite alloy, we further measured the electric resistance under different magnetic fields. Fig. 3 displays the temperature dependent resistivity measured in different magnetic fields for the as-spun sample. The zero-field resistivity increases with increasing temperature (below 260 K), which is different from the typical Gd-based AMs showing negative temperature coefficient of resistivity. And there is no clear change around the lower magnetic transition temperature ~100 K, but exists a shallow minimal around the higher magnetic transition temperature which is suppressed by the external fields. Nevertheless, the two magnetic transitions can be clearly seen from the temperature dependence of MR (=R(H)/R(0)-1), especially under 2 and 5 T, which shows two shallow minima. Similar behavior has been observed in the irradiated sample as shown in the inset of Fig. 3 (b). The MR vs $-\Delta S_m$ plot is shown in Fig. 4(a–d) for the as-spun ribbon. Above the Curie temperature, it is found that $-\Delta S_m$ and MR follow almost a linear relationship for the as-spun sample. Below the low magnetic transition temperature, the $-\Delta S_m$ vs MR obeys a power law relation very well: $MR \propto |-\Delta S_m|^c$, where the c is determined to be around 0.5. Furthermore, irradiation changes the relationship obviously as shown in Fig. 4(e and f), which is sensitive to the external field.

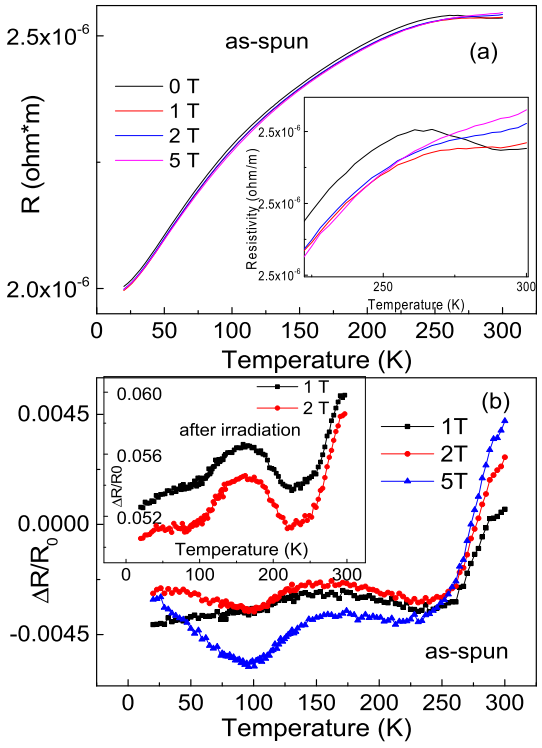

Fig. 3. Temperature dependence of the resistivity under different fields of the as-spun alloy, the inset shows the enlarged part. (b) The temperature dependence of MR under different fields for the as-spun alloy. The inset shows the MR under 1 T and 2 T for the irradiated alloy.

Under 1T, a power law/linear relationship is observed above/below the Curie temperature. But under 2 T, the power law is observed both below and above the Curie temperature. The difference of the MR-MEC relationship between the as-spun and irradiated sample is related to the local structure change and stress relaxation by irradiation. In some crystalline compounds like $CoPt_3$, Tm-Cu(Ag) [30,31], a linear relationship between MR and MEC was observed above, at, and just below T_C. Different relationships were also observed in other crystalline solids [32,33]. Note that in a Gd-based metallic glass ribbon, the $-\Delta S_m$ was reported to show a power-law/linear relationship with MR above/below the Curie temperature [34], which is in contrast with present nanocrystalline/amorphous alloys. The above results indicate that local atomic structure has a significant influence on the relationship between electronic and magnetic properties. At present the underlying mechanism of these correlations is still unclear, which requires more theoretical and experimental investigations.

In conclusion, large magnetocaloric response has been observed in a Gd-based nanocrystalline/amorphous composite with two well separated magnetic transitions, in which the interactions between the amorphous and nanocrystalline phases can be neglected. The magnetocaloric performance can be further improved by Ar irradiation, which is attributed to the stress and heating effects by irradiation (leading to the local structure change around Gd atoms). This demonstrates that the irradiation could be useful to tune the magnetocaloric properties of nanostructured/amorphous materials in a non-homogeneous manner. Different from the conventional annealing, irradiation allows a route to induce localized structural modifications over large surface areas to tune the properties. In addition, it is worthy of noting that, irradiation induced crystallization should be different from thermal crystallization, since strain produced during irradiation has an important impact on the

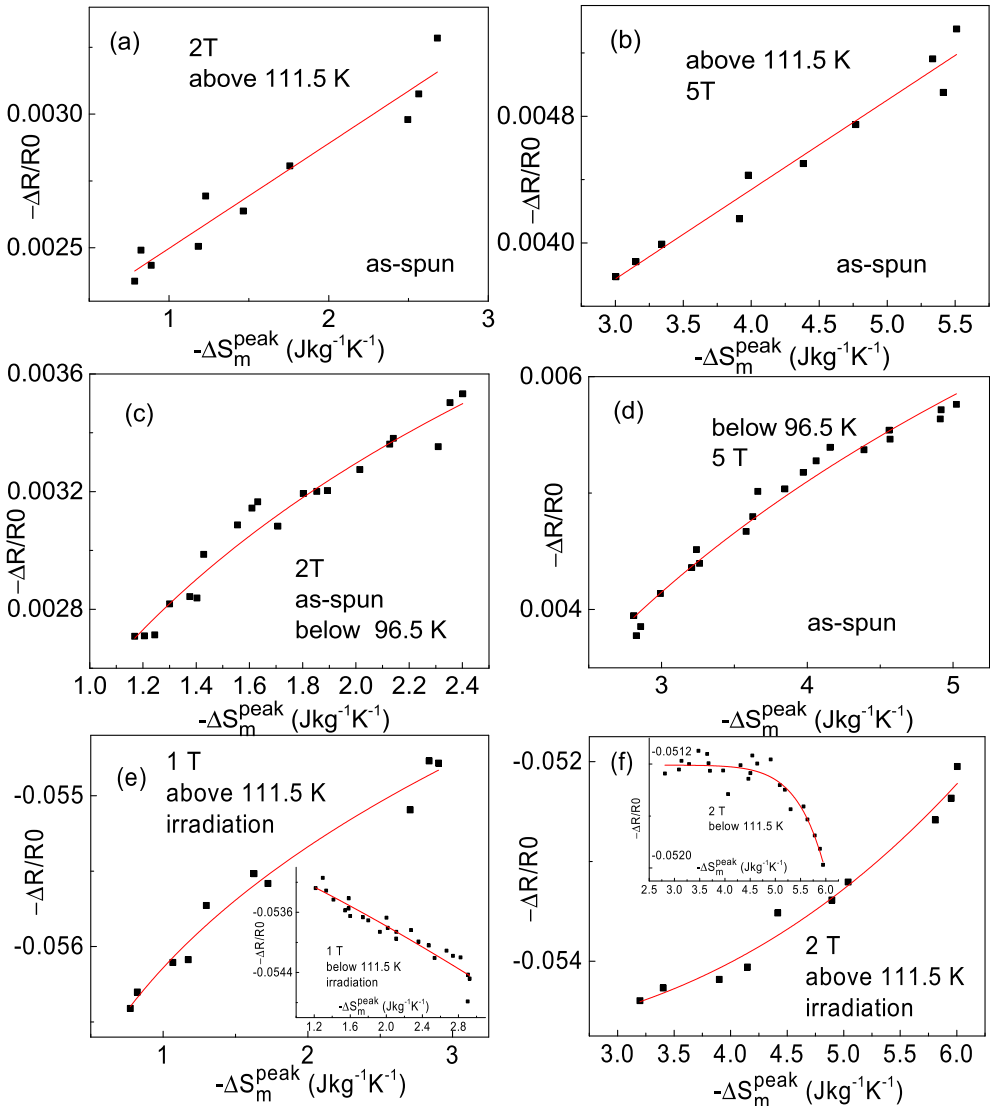

Fig. 4. Relationship between MR and MEC above/below the Curie temperature under different field changes for the as-spun and irradiated ribbons.

crystallized products. The correlation between ΔS_m and MR indicates the magnetoresistance can act as a probe to the MEC in the amorphous/nanocrystalline composites as well as other alloys. Compared with the heat capacity or magnetization measurements to determine ΔS_m, magnetoresistance experiment is faster. These findings reveal new insights on the nature of MEC of amorphous/nanocrystalline composites, and can guide the design of advanced composite materials for magnetic cooling application.

Acknowledgment

This work is supported by the National Natural Science Foundation of China (Grant Nos. 51371127, 51601130, 51274151, 51471050 and 51631003).

References

[1] V. Franco, J.S. Blázquez, J.J. Ipus, J.Y. Law, L.M. Moreno-Ramírez, A. Conde, Prog. Mater. Sci. 93 (2018) 112.
[2] F.X. Hu, B.G. Shen, J.R. Sun, Z.H. Cheng, Phys. Rev. B 64 (2001), 012409.
[3] a O. Tegus, E. Bruck, K.H.J. Buschow, F.R. de Boer, Nature 415 (2002) 150; b V. Provenzano, A.J. Shapiro, R.D. Shull, Nature 429 (2004) 853.
[4] S. Fujieda, A. Fujita, K. Fukamichi, N. Hirano, S. Nagaya, J. Alloys Compd. 408 (2006) 1165.
[5] S.A. Nikitin, et al., Phys. Lett. A 148 (1990) 363.
[6] A. Midya, P. Mandal, S. Das, S. Banerjee, L.S.S. Chandra, V. Ganesan, S.R. Barman, Appl. Phys. Lett. 96 (2010), 142514.
[7] P. Gorria, P. Alvarez, J.S. Marcos, J.L.S. Llamazares, M.J. P erez, J.A. Blanco, Acta Mater. 57 (2009) 1724.
[8] a Q. Luo, D.Q. Zhao, M.X. Pan, W.H. Wang, Appl. Phys. Lett. 88 (2006), 081914; b Q. Luo, D.Q. Zhao, M.X. Pan, W.H. Wang, Appl. Phys. Lett 90 (2007), 211903.
[9] C.F. Sanchez-Valdes, et al., Appl. Phys. Lett. 104 (2014) 212401.
[10] a V. Franco, J.S. Blázquez, A. Conde, Appl. Phys. Lett. 88 (2006), 042505; b V. Franco, R. Caballero-Flores, A. Conde, Q.Y. Dong, H.W. Zhang, J. Magn. Magn. Mater 321 (2009) 1115.
[11] J.T. Huo, D.Q. Zhao, H.Y. Bai, E. Axinte, W.H. Wang, J. Non-Cryst. Solids 358 (2013) 1716.
[12] J. Du, Q. Zheng, Y.B. Li, Q. Zhang, D. Li, Z.D. Zhang, J. Appl. Phys. 103 (2008), 023918.
[13] N.S. Bingham, H. Wang, F. Qin, H.X. Peng, J.F. Sun, V. Franco, H. Srikanth, M.H. Phan, Appl. Phys. Lett. 101 (2012), 102407.
[14] F.X. Qin, et al., Acta Mater. 61 (2013) 1284.
[15] Q. Luo, B. Schwarz, N. Mattern, J. Shen, J. Eckert, AIP Adv. 3 (2013), 032134.
[16] X.G. Zhao, J.H. Lai, C.C. Hsieh, Y.K. Fang, W.C. Chang, J. Appl. Phys. 109 (2011) 07A911.
[17] J. Swierczek, J. Alloys Compd. 615 (2014) 255.
[18] Y. Bao, et al., J. Alloys Compd. 708 (2017) 678.
[19] Q. Luo, B. Schwarz, N. Mattern, J. Eckert, Phys. Rev. B 82 (2010), 024204.
[20] N.S. Bingham, H. Wang, F. Qin, H.X. Peng, J.F. Sun, Appl. Phys. Lett. 101 (2012) 102407.
[21] J.W. Lai, et al., J. Magn. Magn. Mater. 390 (2015) 87.

[22] Q. Zheng, L. Zhang, J. Du, Scripta Mater. 130 (2017) 170.
[23] S. Gorsse, B. Chevalier, G. Orveillon, Appl. Phys. Lett. 92 (2008), 122501.
[24] H. Fu, Q. Zheng, M.X. Wang, Appl. Phys. Lett. 99 (2011) 162504.
[25] L. Tang, K. Peng, Y. Wu, W. Zhang, J. Alloys Compd. 695 (2017) 2136.
[26] H. Oesterreicher, F.T. Parker, J. Appl. Phys. 55 (1984) 4334.
[27] Q. Luo, M. Tang, J. Shen, J. Magn. Magn Mater. 401 (2016) 406.
[28] L. Xia, K.C. Chan, M.B. Tang, Y.D. Dong, J. Appl. Phys. 115 (2014), 223904.
[29] Q. Luo, P.N. Dinh, X. Kou, J. Shen, J. Alloys Compd. 725 (2017) 835.
[30] R. Rawat, I. Das, J. Phys. Condens. Matter 13 (2001) L379.
[31] N. Sakamoto, T. Kyomen, S. Tsubouchi, M. Itoh, Phys. Rev. B 69 (2004), 092401.
[32] J.C.P. Campoy, E.J.R. Plaza, A.A. Coelho, S. Gama, Phys. Rev. B 74 (2006) 2952.
[33] H.H. Potter, Proc. R. Soc. Lond. Ser. A 132 (1931) 560.
[34] Q. Luo, J. Shen, Intermetallics 92 (2017) 79.